

Percolation and jamming in random sequential adsorption of linear segments on square lattice

Grzegorz Kondrat¹ and Andrzej Pękalski²

Institute of Theoretical Physics, University of Wrocław, pl. M. Borna 9, 50-204 Wrocław, Poland
email addresses : ¹ gkon@ift.uni.wroc.pl, ² apekal@ift.uni.wroc.pl

We present the results of study of random sequential adsorption of linear segments (needles) on sites of a square lattice. We show that the percolation threshold is a nonmonotonic function of the length of the adsorbed needle, showing a minimum for a certain length of the needles, while the jamming threshold decreases to a constant with a power law. The ratio of the two thresholds is also nonmonotonic and it remains constant only in a restricted range of the needles length. We determine the values of the correlation length exponent for percolation, jamming and their ratio.

PACS numbers: 05.40.+1, 64.60 Ak

I. INTRODUCTION

The problem of percolation is an old one [1] but still new results appear and some unsolved questions remain [2]. In general site percolation is defined on a d -dimensional lattice where each site can be either occupied with the probability c or empty with the probability $1-c$. Neighboring occupied sites form a cluster. If it is so large that it reaches the two opposite edges of the lattice, e.g. top and bottom, the cluster is said to be percolating. The lowest concentration of occupied sites for which there is a percolating (or spanning) cluster for an infinite lattice is called the percolation threshold c_p [2].

Another realization of the percolation problem is random sequential adsorption (RSA), in which objects (point particles, segments, rectangles etc.) are put on randomly chosen sites and the objects do not move [3]. It is also possible to consider RSA in a continuum [4].

Jamming is a problem related to RSA percolation [3]. Again objects are placed randomly on the lattice sites until a concentration c_j is reached, where there is no room on the lattice for the next object. For point like particles $c_j = 1$, but for spatially extended entities $c_j < 1$. Continuum models of jamming also exist [3].

The RSA models irreversible dissociation [5] and binding of large ligands to polymer chains [6]. Another area of applicability is the deposition of large molecules on solid surfaces, like proteins [7] or macromolecules on biological membranes [8]. The isotropic-nematic transition in the hard rods like polymers has been studied first by Flory [9] and later e.g. in [10]. Spatial organization of needles into a well organized nematic phase is however a different problem, not considered here. General forms of percolation models have a wide range of applications - from chemisorption, spatially disordered systems, porous materials, car parking and ecology [3], to separating the good and bad people at the entrance to Hades [11]. For overview of percolation, jamming and related problems see [3].

In a recently published paper [12] Vanderwalle et al. studied the relation between the two transitions - per-

colation and jamming. They used two kinds of objects - linear segments of length 2 to 10 and square blocks. They have found that the ratio of the two threshold concentrations c_p and c_j is constant $c_p/c_j \approx 0.62$, regardless of the length of the needle.

In the present paper we extend the study of Vanderwalle et al. to larger lattices and longer objects (we consider only linear segments). In particular we shall check the claim that the c_p/c_j ratio does not depend on the length of the needles.

II. THE MODEL

We consider a square lattice of size $L \times L$. On the sites of the lattice we put randomly linear segments (needles) of a given length a , with the constraint that the needles cannot cross each other, although they may touch themselves. We used hard boundary conditions, i.e., the needles may touch the edge of the lattice but they cannot stick out of it - each needle must lay totally inside the lattice. Adopting open boundary conditions does not affect the results.

To achieve simulation efficiency, our algorithm of deposition needles consists of two parts designed for two different regimes. Firstly when the current concentration of the needles is small, we chose randomly, from a uniform distribution, the orientation (vertical or horizontal) and position of the upper left end of the needle to be inserted. If there is enough space on the lattice, the needle is deposited, if not we pass to the next try. After a certain number of adsorption trials we switch to the other regime where the dense routine is applied. A list of all empty sites and orientations still available is made. From that list a site is randomly chosen. We determine the direction of the needle and check whether the needle can be put there. In any case the site is removed from the list. The process is continued till the last item on the list. Such organization saves time, since we avoid to insert needles into densely packed regions.

A cluster is defined as a group of sites linked by the needles. If there is an uninterrupted path between the

top and the bottom of the lattice, the cluster is said to be percolating or spanning, and the concentration of occupied sites defines the percolation threshold c_p . The concentration at which no more needles could be put on the lattice without violating the constraint determines the jamming threshold c_j .

We have considered lattices of sizes $L = 30, 100, 300, 1000, 2500$ and needles of length $a = 1 \dots 2000$. On the smallest lattices only smaller needles were located. Averaging was done over 100 independent runs. We have checked that averaging over 1000 runs did not reduce the error (mean standard deviation - σ) in a marked way.

III. RESULTS

Our main results of the simulations are presented in Figure 1, where the percolation and jamming thresholds, as well as their ratio, are plotted against the length of the needles ($a = 1 \dots 45$). These data are obtained for lattice size $L = 2500$. As convergence and error analysis shows (see below) we can safely accept them as the asymptotic ($L \rightarrow \infty$) values.

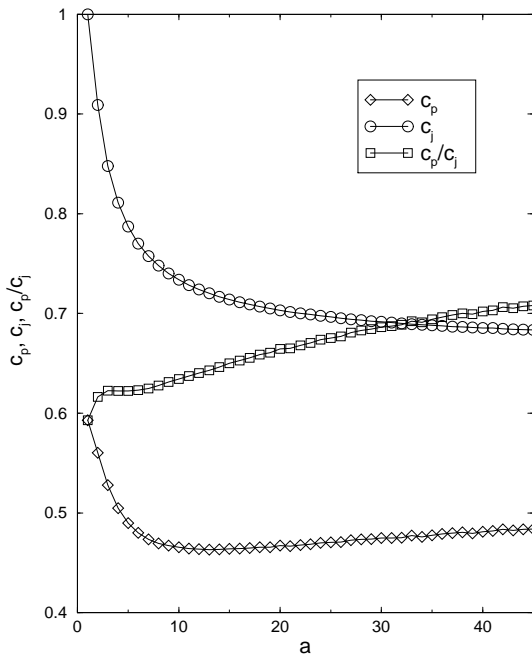


FIG. 1. Thresholds for percolation c_p , jamming c_j and their ratio c_p/c_j versus needles' length, a . Lattice size $L = 2500$. Averaged over 100 samples.

The percolation threshold for $a = 1 \dots 13$ diminishes, then it begins to grow linearly with the slope 0.00071. The minimum value $c_{p \min} = 0.463$ is reached for $a = 13$. As seen in Figure 2, the σ increases with the size of the needles starting from 0.001 ($a = 1$) up to 0.008 ($a = 45$).

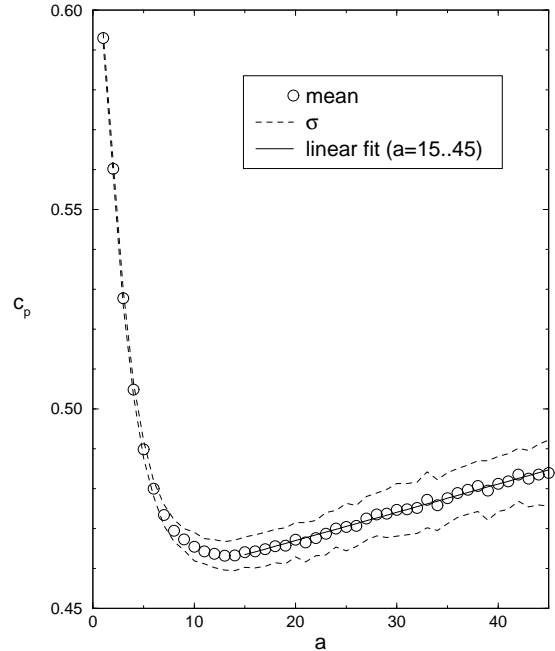


FIG. 2. Percolation threshold c_p versus needles' length a . $L = 2500$, 100 runs. Short needles $a = 1 \dots 45$.

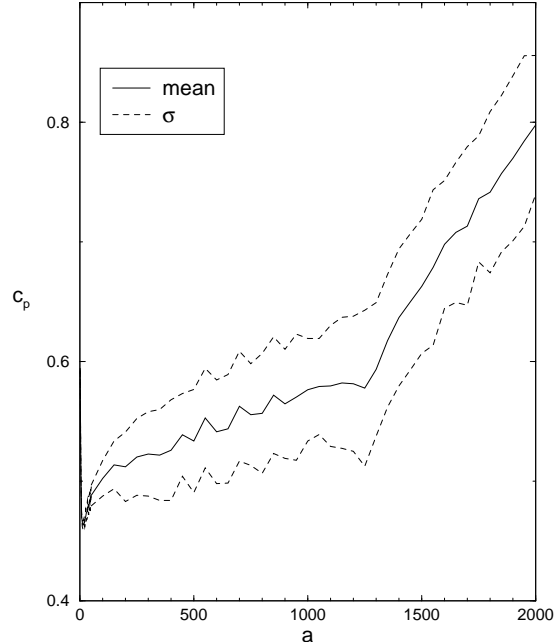


FIG. 3. Percolation threshold c_p versus needles' length a . $L = 2500$, 100 runs. Long needles $a = 1 \dots 2000$.

The increase of the percolation threshold for longer a is however quite clear. The appearance of this novel and unexpected feature is connected with the condition that

the needles may touch themselves but they cannot cross. In the simulations where the restriction has been lifted we observed no minimum but a monotonic decrease. In the model considered here the needles have the tendency to align in parallel not only with respect to the edges of the lattice but also to themselves (see Figures 4 and 5), hence the needles form compact clusters.

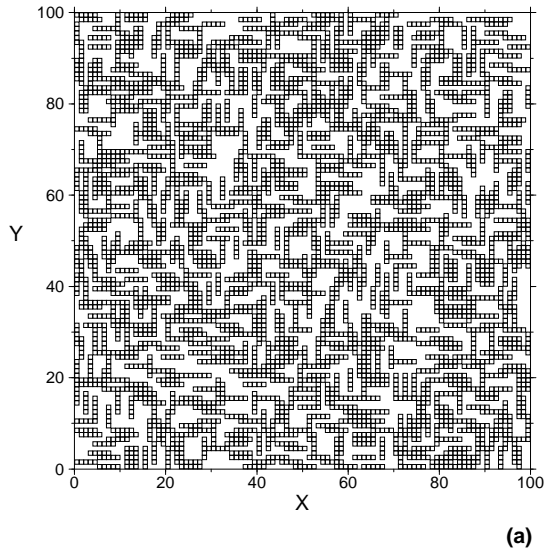


FIG. 4. Snapshot of a spatial distribution of needles at the percolation threshold for $L = 100$, $a = 5$.

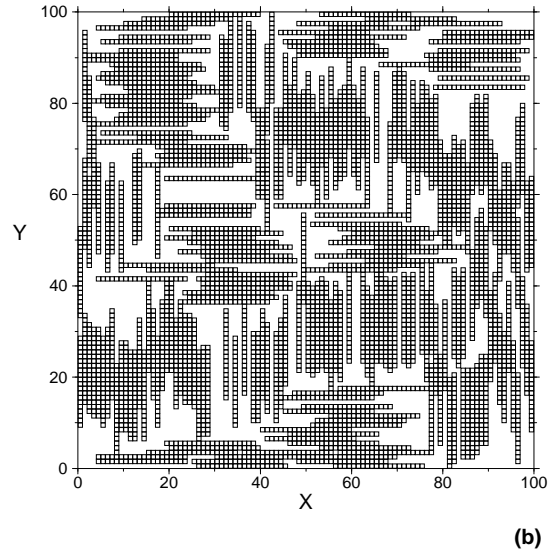


FIG. 5. Snapshot of a spatial distribution of needles at the percolation threshold for $L = 100$, $a = 20$.

In case of horizontally oriented needles in order to move e.g. two steps down, two needles of length a are needed. The longer are the needles the higher is the percentage of occupied sites necessary for passing these two steps. The increase of $c_p(a)$ is to a certain degree compensated by vertically oriented needles, which however also form clusters, thus offering many equivalent ways for percolation. Further simulations for much longer needles indicate continuous increase in c_p , although at a slower rate - see Figure 3.

The jamming thresholds obtained from the simulations have much smaller error than that for percolation and even for $a = 45$ it is below 0.002. Values of c_j , as a function of a , decrease according to a power law (very good fit for all $a \geq 5$) approaching the asymptotic value $c_j^* = 0.66 \pm 0.01$ (see Figure 6):

$$c_j = c_j^* + 0.44 \cdot a^{-0.77}. \quad (1)$$

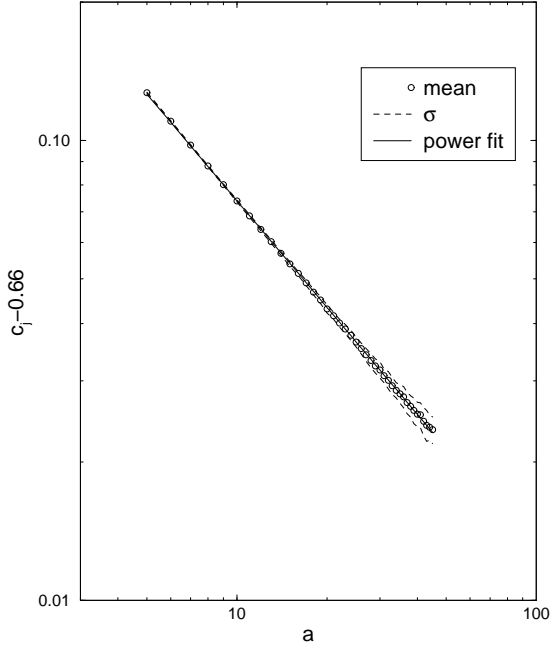


FIG. 6. Jamming threshold c_j versus needles' length a on a log-log plot. $L = 2500$, 100 runs. $a = 5 \dots 45$.

The uncertainty of the exponent derived from the graph analysis equals 0.02. Clearly this behaviour differs essentially from bare power law postulated in [4] :

$$c_j \sim a^{-0.2}, \quad (2)$$

for the continuum (off - lattice) case of RSA of randomly oriented and highly anisotropic (length to wide) rectangles. Their a coincides with our length of needles a . In the discrete case we did not observe the maximum of c_j at $a = 2$ reported in [4]. The reason is that on the lattice the number of possible orientations of the needles is restricted to $z/2$ (where z is the coordination number of the lattice) in contrast to the continuum case. It is interesting that the asymptotic concentration for jamming (for $a \rightarrow \infty$) is 0 off lattice and it remains finite in the discrete case.

Other interesting quantity in our model is the ratio c_p/c_j as a function of a (see Figure 7).

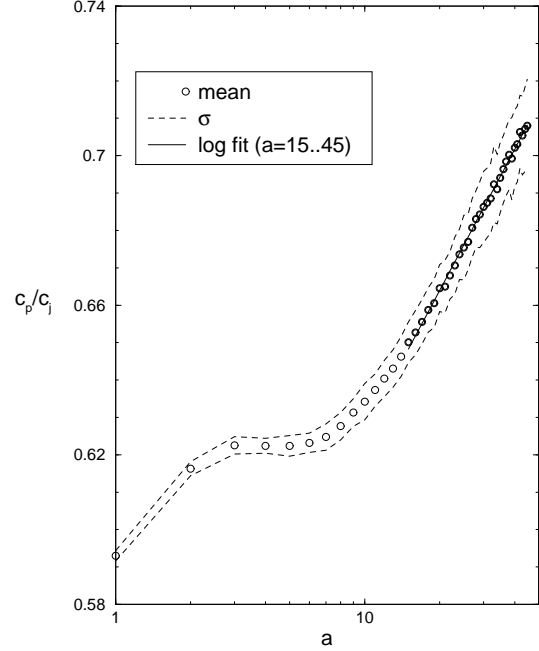


FIG. 7. Percolation to jamming thresholds ratio c_p/c_j versus needles' length a . $L = 2500$, 100 runs. Logarithmic fit for $a = 15 \dots 45$.

It grows for $a = 1 \dots 3$, then it stabilizes till $a = 7$ and then it grows again. The plateau value of $c_p/c_j \approx 0.62$, the constant found in [12]. The growth for longer needles ($15 \leq a \leq 45$) could be fitted by a logarithmic dependence

$$c_p/c_j \sim 0.50 + 0.13 \cdot \log a. \quad (3)$$

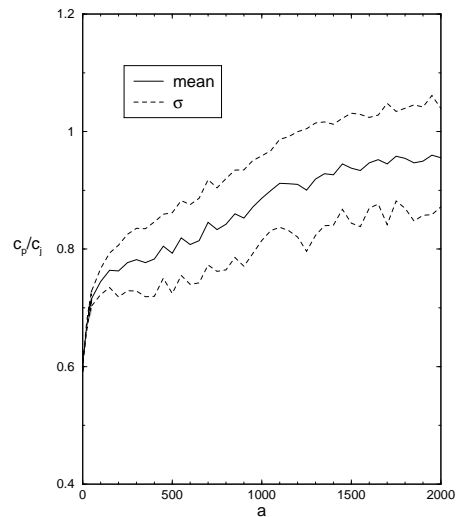


FIG. 8. Percolation to jamming thresholds ratio c_p/c_j versus needles' length a . $L = 2500$, 100 runs. $a = 1 \dots 2000$.

Further simulations for longer needles (see Figure 8) support our claim of monotonic increase in c_p/c_j over wide range of a (even up to $a = 2000$). We may conclude therefore that the universality claimed in [12] holds only in a rather restricted range of $a \in [3, 7]$. As a matter of fact, the value of c_p/c_j for $a > 7$ shown in Table 1 of [12] is greater than those for $a \leq 7$ but the authors attribute it to the finite size effects. This is however most probably just the beginning of the growth of c_p/c_j .

We analyzed the dependence of the obtained thresholds on the lattice size L and needles' length a focusing on convergence. It appeared that for the ratio $a/L < 1/3$ the values of c_p and c_j do not vary much with increasing L (keeping a constant) - see Figures 9 and 10.

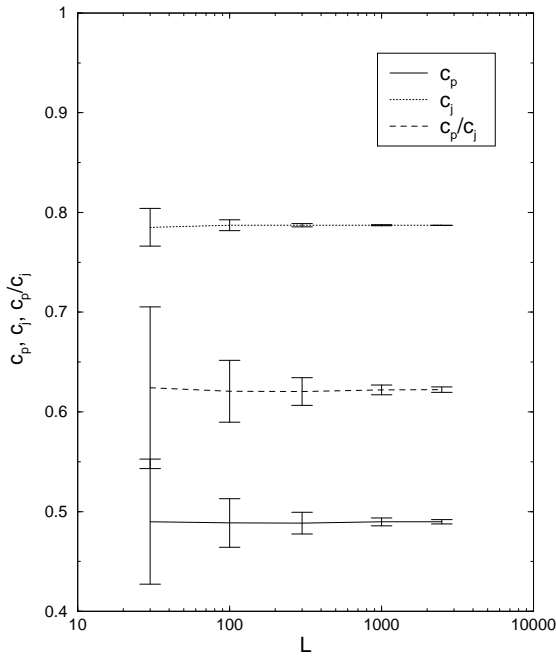


FIG. 9. Convergence analysis of percolation, c_p , jamming thresholds, c_j , and their ratio c_p/c_j , versus lattice size L . 100 runs, $a = 5$.

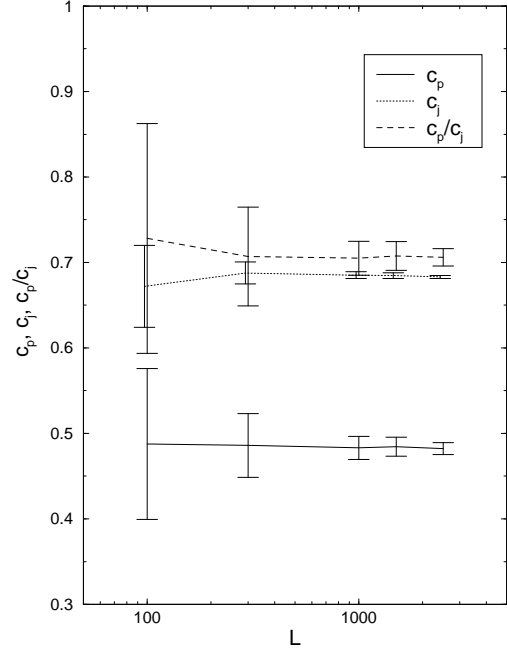


FIG. 10. Convergence analysis of percolation, c_p , jamming thresholds, c_j , and their ratio c_p/c_j , versus lattice size L . 100 runs, $a = 45$.

The error bars (here σ) however decrease rapidly with L , whilst the difference of the thresholds for different lattice sizes is much smaller than the appropriate error. Thus it is safe to take the values of the thresholds from the simulations with $L = 2500$ as the asymptotic (exact) ones.

The finite size effects can clearly be seen in Figure 3, where c_p is drawn against $a = 1 \dots 2000$ for $L = 2500$. At $a = L/2$ we can notice sharp change in the slope of the function $c_p(a)$.

Consider now the dependence of σ of $c_p, c_j, c_p/c_j$ on the lattice size. σ is analogous to the quantity Δ defining in [12] the sharpness of the transition (non-percolating to percolating or non-jammed to jammed). Here however the power law approach to the asymptotic value $p(\infty) - p(L) \sim L^{-1/\nu}$ (cf. formula (3) in [12]) does not hold.

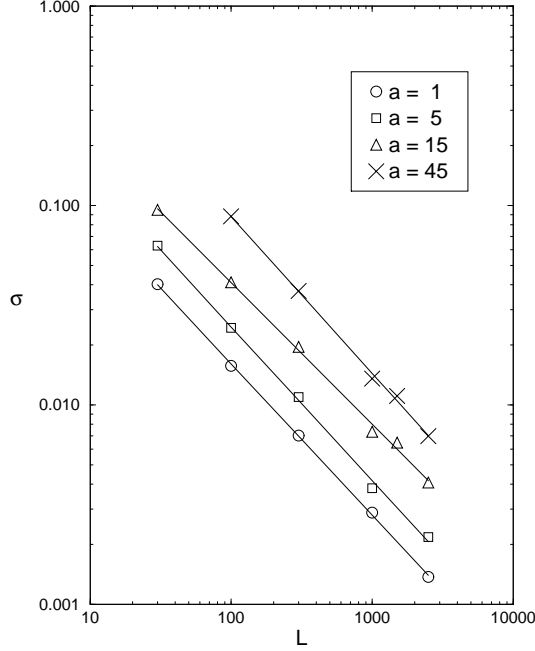


FIG. 11. Deviation analysis. σ versus lattice size L for several values of the needles' length. Percolation.

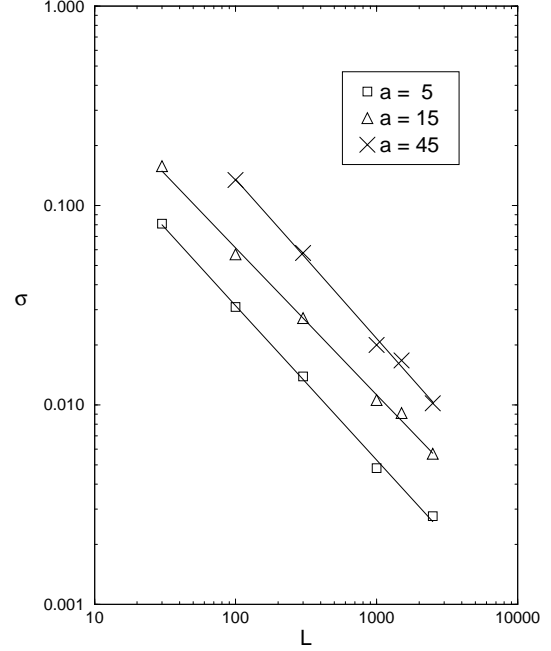


FIG. 13. Deviation analysis. σ versus lattice size L for several values of the needles' length. Percolation to jamming ratio.

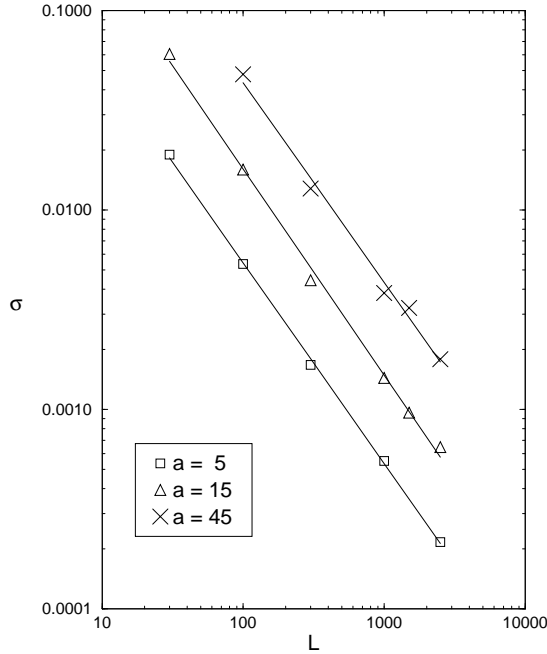


FIG. 12. Deviation analysis. σ versus lattice size L for several values of the needles' length. Jamming.

We have found (see Figures 11 - 13) that the σ for percolation (Δ_p), jamming (Δ_j) and the c_p/c_j ratio (Δ_r) decrease with the lattice size according to the power laws

$$\begin{aligned} \Delta_p &\sim L^{-1/\nu_p}, & 1/\nu_p &= 0.75 \pm 0.05, \\ \Delta_j &\sim L^{-1/\nu_j}, & 1/\nu_j &= 1.00 \pm 0.05, \\ \Delta_r &\sim L^{-1/\nu_r}, & 1/\nu_r &= 0.77 \pm 0.05. \end{aligned} \quad (4)$$

Here ν corresponds to the correlation length exponent [2]

$$\xi \sim |c - c_p|^{-\nu}. \quad (5)$$

These values are, within the error bars, the same for all $a = 1 \dots 45$ and agree with those found by Vanderwalle et al [12]. Also Nakamura [13] found $\nu_j = 1.0 \pm 0.1$ for RSA of square blocks. It seems therefore that the exponents ν are good candidates for universal quantities.

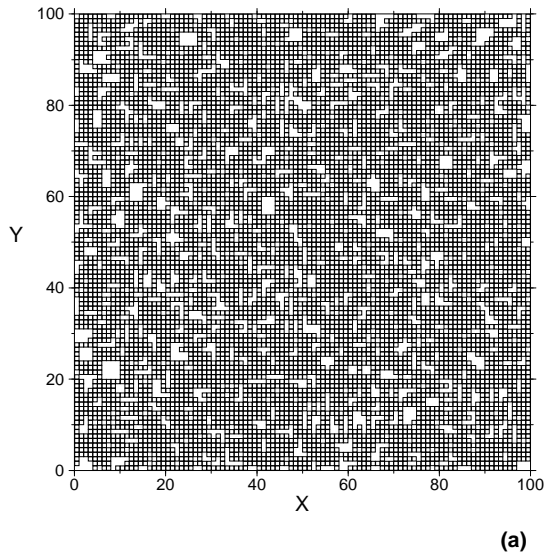


FIG. 14. Snapshot of a spatial distribution of needles at the jamming threshold for $L = 100$, $a = 5$.

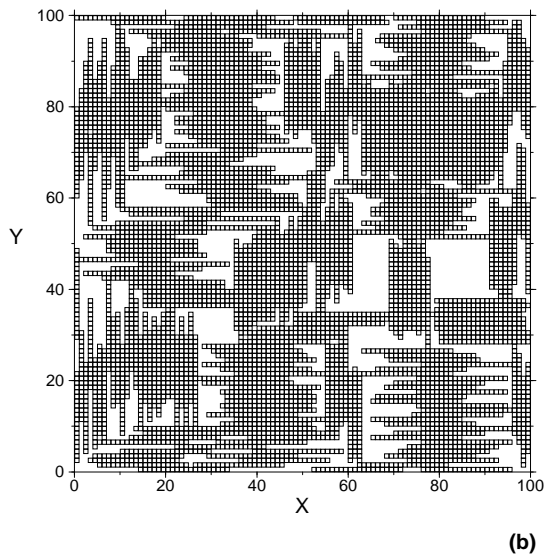


FIG. 15. Snapshot of a spatial distribution of needles at the jamming threshold for $L = 100$, $a = 20$.

Examples of spatial arrangements of shorter ($a = 5$) and longer ($a = 20$) needles on a lattice 100×100 are shown in Figures 4 and 5 (percolation) and in Figures 14

and 15 (jamming). Analysis based on examination of different runs shows some regularity in the needles distribution – we have found that the needles near the edges have the tendency to stick along the borders. Longer needles, for obvious reasons, form clusters of parallel alignment, as was already observed in [12].

IV. CONCLUSIONS

We have performed extensive simulations of RSA using linear segments of size $a = 1 \dots 45$ on square lattice sites. We have found that the percolation threshold is a nonmonotonic function of a , having a minimum due to parallel orientation of the needles, at $a = 13$, while the jamming threshold decreases to a non-zero constant with a as a power law. The ratio of the two thresholds is nonmonotonic too - after initial growth it stabilizes for some values of a , and then it grows logarithmically. Whether the asymptotic value is equal to one or below it is an interesting question. To answer it unequivocally is unfortunately beyond our computing power. The values of the correlation length exponent ν , for percolation, jamming thresholds and the ratio of the two, do not depend on the length of the needles and they are, within the error bars, equal to those found elsewhere [12] [13] for deposition of needles, rectangles or squares.

ACKNOWLEDGMENTS

We are grateful to M.Droz, J.O. Indekeu, Z. Koza and N. Vandewalle for helpful comments.

-
- [1] J.M. Hammersley, Proc.Phil.Soc.Math.Phys.Sci. **53**, 642 (1957).
 - [2] D. Stauffer, Physica **A 242**, 1, (1997),
D. Stauffer and A. Aharony *Introduction to Percolation Theory*, Taylor & Francis, London 1994.
 - [3] J.W. Evans, Rev.Mod.Phys. **65**, 1281 (1993).
 - [4] R.D. Vigil and R.M. Ziff, J.Chem.Phys. **91**, 2599 (1989).
 - [5] A.C. Balazs and I.R. Epstein, Biopolymers **23**, 1249 (1984).
 - [6] E.A. Boucher, Trans.Far.Soc. **69**, 1839 (1973).
 - [7] J.J. Ramsden, Phys.Rev.Lett. **71**, 295 (1993).
 - [8] L. Finegold and J.T. Donnell, Nature **278**, 443 (1979)
 - [9] P.J. Flory, Proc.R.Soc. London, Ser. A **234**,73 (1956).
 - [10] H. Weber, W. Paul and K. Binder, Phys.Rev. **E 59**, 2168 (1999).
 - [11] C. Domb, E. Stoll and T. Schneider, Contemp.Phys. **21**, 577 (1980).

- [12] N. Vanderwalle, S. Galam and M. Kramer, Eur.Phys.J.
B 14, 407 (2000).
- [13] M. Nakamura, J.Phys. **A: Math.Gen.** **19**, 2345 (1986).